Comparisons of Scatterometer and TAO Winds Reveal Time-Varying Surface Currents for the Tropical Pacific Ocean*

KATHRYN A. KELLY AND SUZANNE DICKINSON

Applied Physics Laboratory, University of Washington, Seattle, Washington

GREGORY C. JOHNSON

NOAA/Pacific Marine Environmental Laboratory, Seattle, Washington

(Manuscript received 8 January 2004, in final form 11 October 2004)

ABSTRACT

The differences between Tropical Atmosphere Ocean (TAO) anemometer and QuikSCAT scatterometer winds are analyzed over a period of 3 yr. Systematic differences are expected owing to ocean currents because the anemometer measures absolute air motion, whereas a radar measures the motion of the air relative to the ocean. Monthly averaged collocated wind differences (CWDs) are compared with available near-surface current data at 15-m depth from drifters, at 25-m depth from acoustic Doppler current profilers (ADCPs), and at 10-m depth from current meters and with geostrophic currents at the surface from the TOPEX/Poseidon radar altimeter. Because direct current observations are so sparse, comparisons are also made with climatological currents from these same sources. Zonal CWDs are in good agreement with the zonal current observations, particularly from 2°S to 2°N where there are strong currents and a robust seasonal cycle, with the altimeter-derived anomalous currents giving the best match. At higher latitudes there is qualitative agreement at buoys with relatively large currents. The overall variance of the zonal component of the CWDs is reduced by approximately 25% by subtracting an estimate of the zonal currents. The meridional CWDs are nearly as large as the zonal CWDs but are unpredictable. The mean CWDs show a robust divergence pattern about the equator, which is suggestive of Ekman currents, but with unexpectedly large magnitudes.

Coefficients for estimating climatological zonal surface currents from the altimeter at the TAO buoys are tabulated: the amplitudes and phases for the annual and semiannual harmonics, and a linear regression against the Southern Oscillation index, are combined with the mean from the drifter currents. Examples are shown of the application of these estimators to data from SeaWinds on the Midori satellite. These estimators are also useful for deriving air–sea fluxes from TAO winds.

1. Introduction

The radar scatterometer measures backscatter from centimeter-scale waves caused by the wind blowing over the ocean; when ocean and atmosphere move together, no waves are generated and no wind is measured. An anemometer, on the other hand, measures the motion of the air relative to a fixed platform. When the wind blows against (with) the surface currents, the scatterometer will measure higher (lower) wind than an anemometer on a buoy. If ocean currents are the dominant source of discrepancies between the two wind measurements, then the difference (anemometer minus scatterometer) should agree with estimates of the ocean surface currents. Differences between the wind vectors from the Tropical Atmosphere Ocean (TAO) buoys and from the SeaWinds scatterometer are compared here with time-varying ocean surface currents over a 3-yr period beginning with the start of the QuikSCAT mission in July 1999.

For purposes of computing air–sea fluxes, the measurement of the relative motion by the scatterometer has an advantage over an anemometer wind. In bulk

* Pacific Marine Environmental Laboratory Contribution Number 2648.

Corresponding author address: Dr. Kathryn A. Kelly, Applied Physics Laboratory, University of Washington, Box 355640, Seattle, WA 98195.
E-mail: kkelly@apl.washington.edu

parameterizations (e.g., Liu et al. 1979), surface stress τ and all other air–sea fluxes are a function of the difference between the wind at a reference height U and the current at the ocean surface U_s, as

$$\tau = \rho C_D |U - U_s|(U - U_s). \quad (1)$$

The wind derived from the scatterometer backscatter represents the relative motion, $U - U_s$. To derive stress from an anemometer wind or from any other absolute wind measurement, it is necessary to subtract an estimate of the ocean surface current. The relative motion, $U - U_s$, is also needed for other bulk flux formulas. The ocean currents are frequently neglected in the bulk formula, because ocean surface currents are not readily available; however, a combination of weak winds and strong currents will give large errors in these flux estimates.

Previous comparisons between TAO and scatterometer winds with currents using relatively small amounts of data suggested an important role for currents in the difference. Collocated wind differences (CWDs) from the National Aeronautics and Space Administration (NASA) Scatterometer (NSCAT) and TAO anemometers showed qualitative agreement with currents from a single current meter on the equator over a 7-month period, as currents reversed during the onset of the 1997 ENSO warm event (Dickinson et al. 2001). Similarly, good agreement was found between QuikSCAT winds and currents from an acoustic Doppler current profiler (ADCP) mounted on a ship servicing the TAO array, averaged over a 3-week period (Kelly et al. 2001). In the comparison with QuikSCAT winds, currents in the South Equatorial Current (SEC) were about 1.2 m s^{-1} westward and currents in the North Equatorial Countercurrent (NECC) were about 0.6 m s^{-1} eastward over the short period examined. Neglect of these strong equatorial currents in this region of relatively weak winds (5–7 m s^{-1}) was estimated to cause errors in stress of 25%–50% and even larger errors in wind stress curl.

Here, we compare 3 yr of CWDs with surface currents at most of the TAO buoys (Fig. 1). The CWDs, which are computed from the difference of two observations, are likely to be noisier than either; in fact, if the error variance for the anemometer is ϵ_a^2 and the error variance for the scatterometer is ϵ_s^2, then the error variance for the current estimate is $\epsilon_a^2 + \epsilon_s^2$, assuming these errors are uncorrelated. Therefore, it was necessary to edit and temporally average the CWDs for the comparisons.

The goals of this analysis are 1) to demonstrate that systematic differences between (zonal) TAO anemometer and QuikSCAT winds are from time-varying ocean currents, 2) to find (and provide) appropriate current estimators to convert between the relative scatterometer and absolute anemometer winds, and 3) to demonstrate the need to include ocean currents in anemometer/scatterometer validation studies.

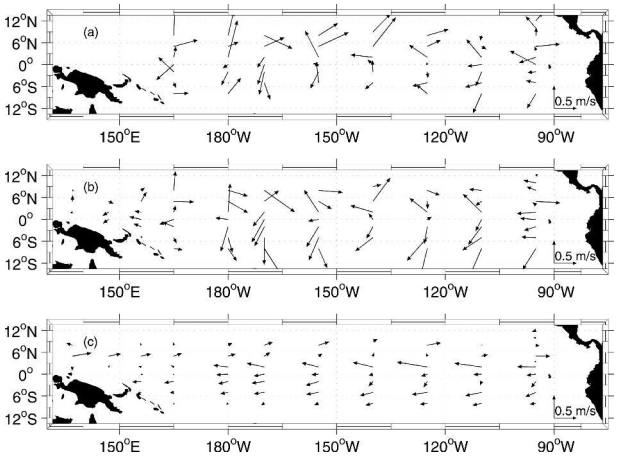

FIG. 1. Estimated mean currents. Difference between TAO and QuikSCAT winds for (a) collocated pairs of vectors from Jul 1999 to Aug 2002 and (b) all daily TAO winds and QuikSCAT winds from gridded fields for Jul 1999–Aug 2003. (c) Mean currents from 15-m-deep drifters at the TAO mooring locations.

Although TAO buoys are not used in the calibration of the scatterometer model function (see, e.g., Wentz and Smith 1999), which relates direction and speed to radar backscatter, they are used to "validate" the winds. The model function is based on global collocated backscatter with several months of wind vectors from numerical weather prediction models; the calibration is a highly overdetermined problem with most of the winds from regions of weak ocean currents. To illustrate the independence of the buoy and scatterometer winds, we note that the *European Remote Sensing Satellite-1* (*ERS-1*), NSCAT, and QuikSCAT scatterometers all showed systematic direction biases to the right of the TAO anemometers of approximately 9°–11°, a remarkable consistency. Subsequent analyses of the accuracy of the ATLAS anemometers revealed a 6.8° bias to the left (Freitag et al. 2001), accounting for much of what was observed by the scatterometers. (This direction error has been corrected in the TAO winds.)

Anemometer winds are used to check the scatterometer speed and direction accuracy ("validation"), and, therefore, it is critical that we understand the nature of the differences in the measurements. In the validation of the NSCAT model function, initial TAO buoy/NSCAT comparisons suggested that the scatterometer winds were too low by about 0.5 m s^{-1}. However, after equatorial currents reversed early in 1997, scatterom-

eter winds appeared to be too high, as would be expected for a relative motion measurement, demonstrating the need to include ocean currents in the comparisons. In the QuikSCAT validation, after removing the measured currents in the CWDs, the model function bias was found to be a negligible 0.1 m s^{-1} (Kelly et al. 2001).

The need for a conversion between buoy and scatterometer winds also arises in the evaluation of flux products. In bulk formulas for estimating latent and sensible heat fluxes, for example, the relative motion $\mathbf{U} - \mathbf{U}_s$ is also needed. At 140°W on the equator, where current measurements are available, latent heat flux estimated with and without these energetic ocean currents had a seasonally varying difference with amplitude of about 7 W m^{-2} and a mean of 2 W m^{-2} (M. Cronin 2004, personal communication). To determine, for example, whether the use of scatterometer winds improves air–sea flux products, as in recent studies by Yu et al. (2004), an accurate comparison with fluxes from a bulk formula at a TAO buoy would also require a current estimate (few TAO buoys have current meters).

2. Collocated wind vectors

The TAO buoys used in this study are located in the equatorial Pacific Ocean bounded by 8°S, 12°N, 165°E, and 95°W. High-resolution TAO buoy data were collected from the beginning of the QuikSCAT mission, July 1999 through August 2002. The buoy data include zonal and meridional wind components, air temperature, sea surface temperature, and relative humidity. The sampling rate for all variables except the sea surface temperature is 2 Hz, with a sampling period of 2 min. Data are recorded every 10 min. The sea surface temperature data are instantaneous measurements taken once every 10 min. The winds, which are measured at a height of 4 m above the ocean surface, are converted to a 10-m height in a neutrally stratified atmosphere using the standard LKB algorithm (Liu et al. 1979). The 6.8° wind direction bias (Freitag et al. 2001) has been removed from the TAO data. TAO winds are temporally averaged to give hourly winds.

QuikSCAT scatterometer wind speed and direction data [standard L2B product from Physical Oceanography Distributed Active Archive Center (PO.DAAC)] (Wentz and Smith 1999; Huddleston et al. 1996) were collected over the 3-yr time period. The scatterometer data are calibrated to approximate a wind at 10 m above the ocean surface in a neutrally stratified atmosphere and have a spatial resolution of 25 km. Data pairs were considered collocated when the scatterometer cell center was within 25 km of a buoy and the time difference was less than 30 min, giving a unique pairing with the hourly TAO winds.

The collocated pairs were screened for rain, wind direction, and wind speed. The rain screen was performed using collocated rain estimates derived from the Special Sensor Microwave Imager (SSM/I) (courtesy of Remote Sensing Systems). The rain estimates consist of a rain rate (or designation of "no rain") and the time difference between the SSM/I and the scatterometer measurement (maximum of 3 h). Because we only used CWDs for which there was a rain estimate indicating "no rain detected within 50 km" of the scatterometer vector, there was a trade-off between reducing rain contamination (and therefore the variance of the CWDs) by selecting a short time difference and the amount of data available for our analysis. We examined the variance of the CWDs for maximum time differences of 30, 60, 120, and 180 min; the CWD variance for the less-stringent 180-min time window was only a few percent higher than the variance for the 30-min time window, but the number of CWDs was double that for the 30-min window. The negligible increase in variance suggests that using the less restrictive 3-h time window does not degrade the scatterometer wind quality. Therefore, to maximize the amount of data for analysis, a collocated buoy–scatterometer pair was included if there was an SSM/I estimate within 3 h of the scatterometer measurement that indicated no rain was present.

The scatterometer model function gives up to four possible wind vectors, owing to the similarity of the backscatter from different viewing geometries. To ensure that the correct scatterometer vector was selected, the collocated pair was retained only if the difference in the wind directions between buoy and scatterometer was less than 60°. Last, if the buoy wind speed was 3 m s^{-1} or less the pair was excluded owing to the difficulty of both sensors in measuring directions for low wind speeds. Of the initial collocations, 10% had buoy wind speeds below the threshold, 6% had directional differences that were too large, and 18% had no SSM/I flag within 3 h or the SSM/I flag indicated rain. Overall, 74% of the pairs met the above requirements, resulting in a dataset of 28 031 collocated wind pairs.

Tropical Pacific Ocean CWDs were estimated by subtracting QuikSCAT scatterometer wind vectors from collocated TAO vectors at 56 TAO buoys. Even after the screening described above, the screened CWDs were quite noisy. To reduce the noise, CWDs with speeds of 2 m s^{-1} or greater were removed, as these represent unrealistically large values for ocean currents and were suspected to be contaminated by a

noise source, such as undetected rain. In addition, a 2-month running mean at monthly intervals was computed for the zonal and meridional components and three-standard-deviation outliers from these means were removed. These criteria eliminated 15% of the remaining data. The 2-month running mean was computed on the remaining CWDs, and these monthly means were used for comparisons with ocean currents.

3. Current observations

There are several sources of near-surface velocity measurements available for comparisons: moored and shipboard ADCPs, drifters, one current meter, and altimetric sea surface height. Moored ADCP data were available at four equatorial buoys in our domain. A single current meter at 110°W on the equator measured 10-m currents for a few months in 2001, allowing another comparison.

Because so few direct current measurements were available at the TAO buoys during our study period, we used current estimates from the other data sources. Currents at 15 m from the drogued drifters of the Global Drifter Program were daily averaged and fit to a function in time and space (Johnson 2001). The mean, annual, and semiannual harmonics, and an SOI regression coefficient for both zonal and meridional currents were estimated at the TAO buoy locations from over two decades of data. From the zonal coefficients we constructed a climatological drifter current time series.

We also examined current estimates from shipboard ADCP data from the shallowest depth at 25 m. Climatological zonal velocities were constructed from 172 longitudinal transects of shipboard ADCP data from 1985 though 2001 based on a regression analysis (Johnson et al. 2002). Meridional ADCP currents are badly aliased by sparse sampling in the presence of strong tropical instability waves (TIWs), and the resulting climatological meridional estimates may be weak.

Sea surface height (SSH) data measured by the TOPEX/Poseidon altimeter were used to compute anomalous geostrophic ocean surface currents, with the following set of equations:

$$u_g = \frac{-g}{f}\frac{\partial \eta}{\partial y}, \qquad v_g = \frac{g}{f}\frac{\partial \eta}{\partial x}, \tag{2}$$

where η is the SSH anomaly and f is the Coriolis parameter. At the equator, where f is zero, a revised formulation was used for the zonal currents, as

$$\beta u_g = -g\frac{\partial^2 \eta}{\partial y^2}, \tag{3}$$

where $\beta = \partial f/\partial y$ (Jerlov 1953).

We used SSH data with a resolution of 6° × 6° × 0 days, mapped to a 1° × 1° × 10 day grid, centered on the half degree. The coarse spatial resolution is set by the 3° altimeter track spacing. The computation of geostrophic velocity using (2) becomes quite sensitive to noise in the SSH near the equator (as f approaches zero). In addition, geostrophic velocities may exceed the actual velocities (Lagerloef et al. 1999; Bonjean and Lagerloef 2002), because the dynamical balances, even as far as 2° from the equator, are not simple.

Therefore, to obtain velocity estimates we used the following procedure. Geostrophic velocities were computed using (2) and centered differences on the half-degree grid down to a latitude of 2.5°. SSH was then regridded to a 0.5° grid near the equator to allow a computation of the velocity on the equator using (3) and a centered difference. Then, at each 10-day interval and at each longitude, the geostrophic velocities from 4.5°S to 4.5°N, combined with the estimate on the equator, were interpolated to the half-degree grid using overdetermined biharmonic splines, which give a smooth estimate without the problematic overshoot of an unconstrained spline (Sandwell 1987). This procedure resulted in slightly smaller geostrophic velocities at 2°S and 2°N than the direct geostrophic calculation using (2).

To compare with the winds at each TAO buoy, the four velocity time series surrounding each buoy location were averaged. Monthly velocity estimates were smoothed using a 2-month running mean. We used the entire record of the altimeter data (10 yr) to compute the climatological current estimates as described below.

An equivalent relationship to (3) can be derived for the meridional component, which includes higher derivatives of the SSH data and is therefore noisy. However, it was not used because, as discussed below, meridional currents do not appear to be geostrophic.

4. Comparisons of the means

The 3-yr mean CWDs (Fig. 1a) have a similar pattern to that found by Quilfen et al. (2001). To determine to what extent this CWD pattern was affected by using a relatively small subset of the wind data (collocated pairs), we compared the difference of the TAO daily winds and the QuikSCAT daily winds derived from gridded maps (Fig. 1b) (Kelly et al. 1999). In both cases, the annual and semiannual harmonics were first removed before computing the mean to prevent the

seasonal cycle for partial years from biasing the estimate. The mean wind difference maps are quite similar overall, suggesting that the set of CWDs is sufficiently large to give a robust estimate of the difference field.

The CWDs are compared with the means from the climatological drifter estimates in Fig. 1c. The zonal CWD and drifter mean currents are similar: predominantly westward along the equator (South Equatorial Current) and predominantly eastward at 5° and 8°N (North Equatorial Countercurrent), with magnitudes of about 0.5 m s^{-1}. However, there are much larger meridional components in the CWDs than in the drifter means. Both are, in the sense of an Ekman divergence, driven by easterly trade winds. The mean CWDs are far more divergent about the equator than the mean drifter currents. Given the differences in the mean components, we discuss the comparisons of each component separately below.

5. Zonal comparisons

We present the time series of zonal CWDs and the zonal velocity observations described above at each buoy location, with plots laid out geographically (upper panels of Fig. 2). Plots from a buoy are shown if the CWDs are available for at least two-thirds of the 3-yr record. Missing buoy winds generally limit the number of collocations. At most buoys only the geostrophic current anomalies are available. Geostrophic velocity estimates have zero mean and are therefore offset from the CWDs because they are derived from SSH anomalies relative to a 10-yr record mean. The CWD and geostrophic velocity amplitudes are quite similar for 2°S–2°N. The CWDs show good agreement, particularly in the seasonal cycle, with all the observed zonal velocities. At 170°, 140°, and 110°W on the equator, where some moored ADCP data are also available, all of the velocity estimates are quite similar in phase and in magnitude. There is also good agreement with the 10-m currents at 110°W on the equator. The comparison at 140°W is enlarged (Fig. 3) to highlight the long ADCP record.

To allow comparisons with the sparse drifter and shipboard ADCP data, climatological current estimates were computed (lower panels of Figs. 2 and 3). The drifter estimator (Johnson 2001) consists of a mean, an annual and a semiannual harmonic, and a factor correlated with the Southern Oscillation index (SOI). The ADCP estimator has only a mean and an annual harmonic. The advantage of using estimators is that a current estimate can readily be derived for any TAO buoy at any time, if there are no concurrent velocity observations.

A similar estimator is derived from the geostrophic currents by regressions, using

$$U_s(t) = a_1 \cos(2\pi t/T + \phi_1) + a_2 \cos(4\pi t/T + \phi_2) + b\,\mathrm{SOI} + c, \quad (4)$$

where the coefficients a_1, ϕ_1, a_2, and ϕ_2 are the amplitude and phase for the annual and semiannual harmonics, b is derived from a linear regression against the SOI, and c is the mean. The time t is in days ($t = 0$ corresponds to the start of any given year), $T = 365.25$, and the SOI is interpolated to the times t. We use SSH data for nearly 10 yr (November 1992 through the middle of 2002) to derive the coefficients. Because the geostrophic currents lack a mean, the drifter mean is used in the altimeter estimator.

The CWDs and the velocity data tend to be larger than the climatological estimators, which are derived from regressions. Of the three estimators, the one derived from the altimeter (a surface velocity estimate with a long and complete record) generally has the largest amplitudes, followed by the drifter, with the ADCP estimates having the smallest amplitudes. The reduction in amplitudes for the ADCP and drifter estimators is due in part to the need to fit the sparse data to a spatial function.

Statistics of the comparisons between CWDs and currents are included in Table 1, which gives the fraction of the variance ("skill") in zonal CWDs described by three different current estimators. Skill is defined here as

$$\mathrm{skill} = 1 - \frac{\langle \epsilon^2 \rangle}{\sigma^2}, \quad (5)$$

where the error ε is the estimated current minus the CWD, σ^2 is the variance of the CWD, and $\langle\cdot\rangle$ is the ensemble average. In this context, the skill represents the reduction in CWD variance that results from subtracting a given ocean current estimator. The skill, or variance reduction, is given instead of a correlation because it is a more stringent test, penalizing errors in both the mean of the estimator and its amplitude; an estimator that is much too small, for example, can have a high correlation, but it will have a low skill (a small reduction in CWD variance).

Skill is 23% for the drifters overall and 17% for the altimeter (with the drifter mean). The ADCP estimator has no significant skill. Although the skill of the drifter estimator is larger than that for the altimeter, the amplitudes of the altimeter estimates are much closer to the amplitudes of the CWDs. The skill is quite sensitive to the mean difference between the CWDs and the estimator. The drifter means are more westward than the means of the CWDs by an average of 0.09 m s^{-1}.

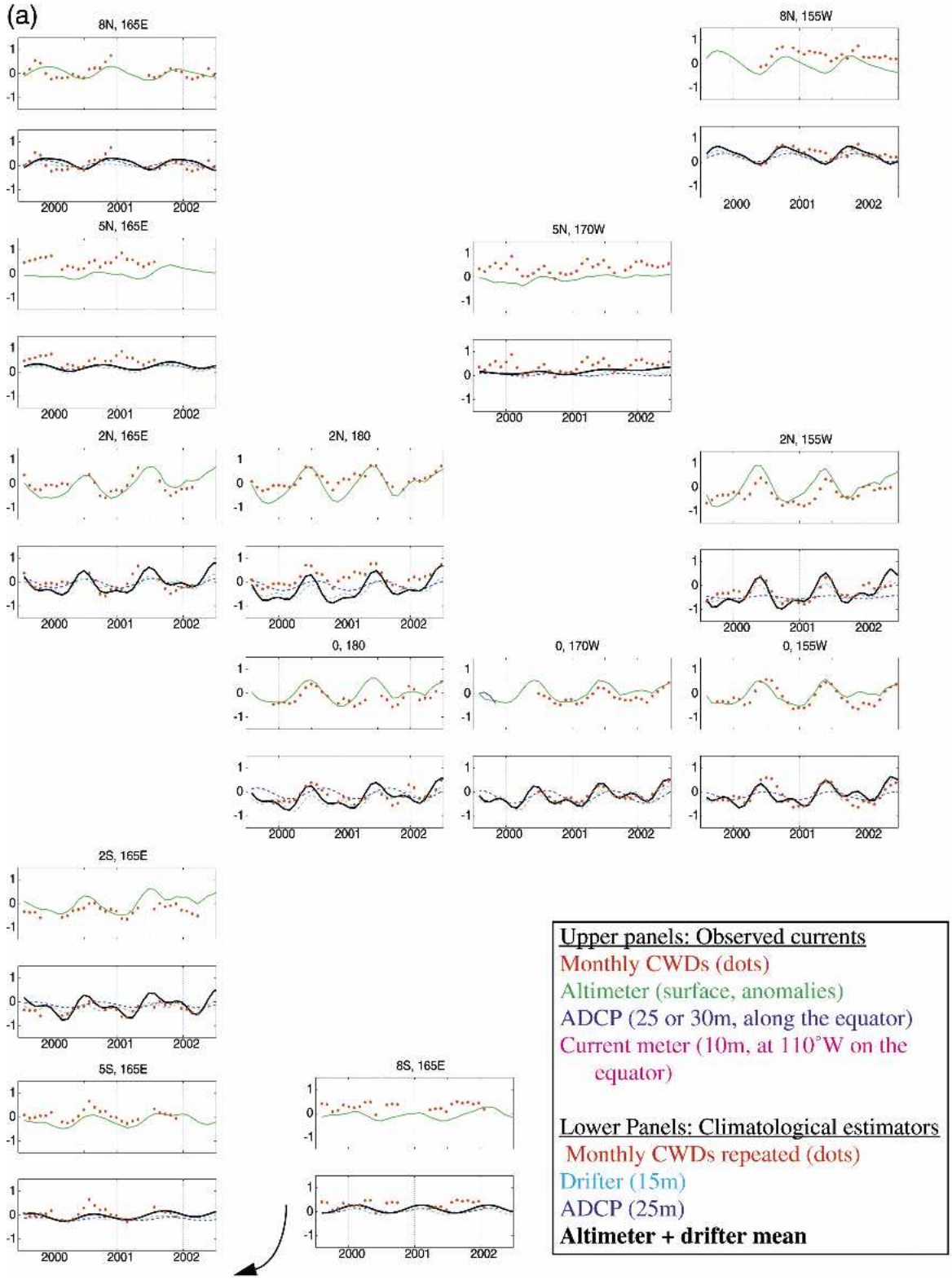

FIG. 2. Zonal wind differences and velocities at TAO buoys. Panels are laid out geographically to represent TAO buoy locations. (top) Monthly CWDs (red dots), geostrophic current anomalies (green), ADCP (blue), and current meter (magenta) on the equator at 110° and 140°W. Geostrophic currents have zero mean. (bottom) Monthly CWDs (repeated), current estimators from ADCP (blue dashed), drifters (cyan dashed), and geostrophic with drifter mean (black). Units: m s^{-1}.

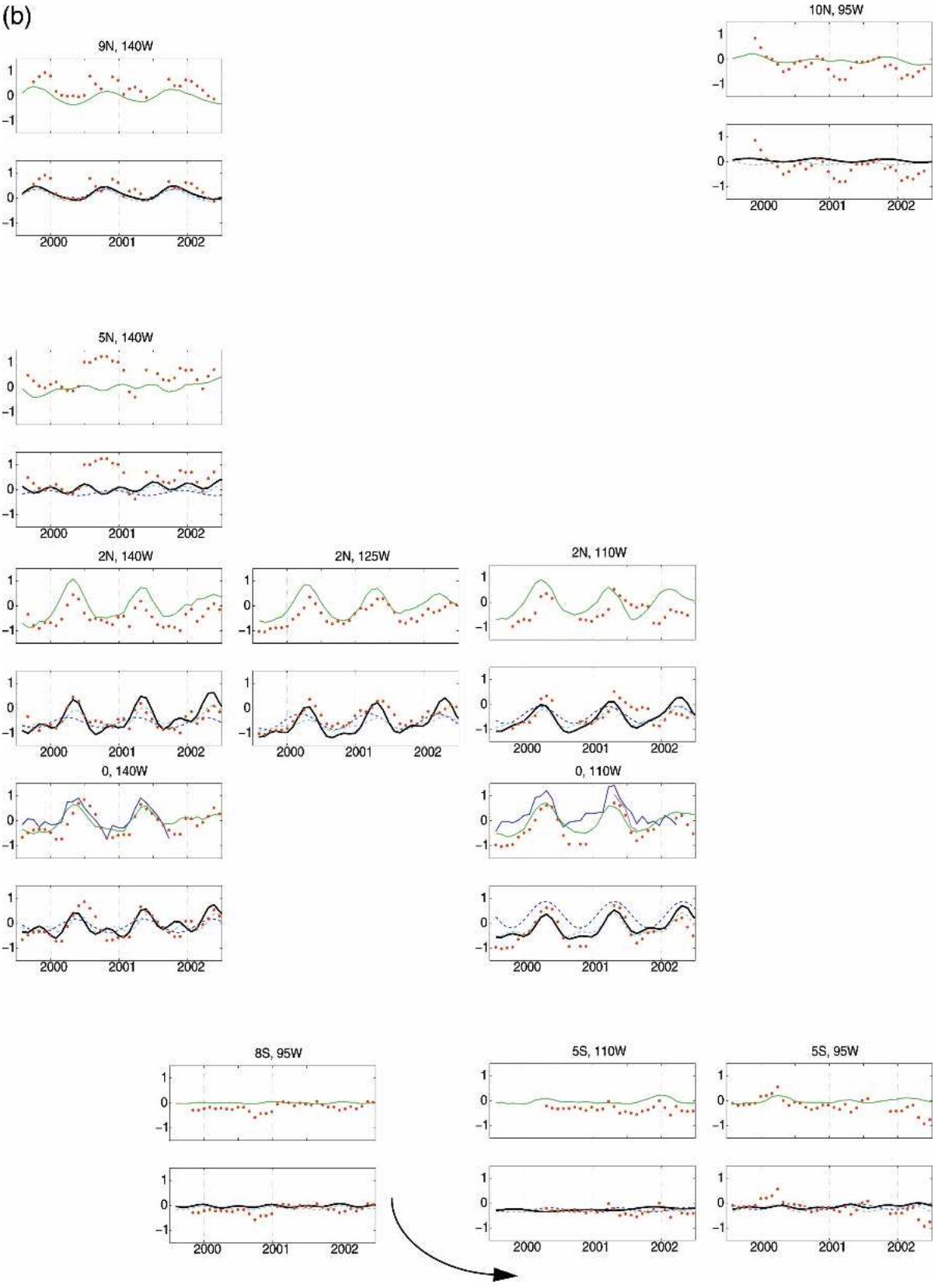

FIG. 2. (*Continued*)

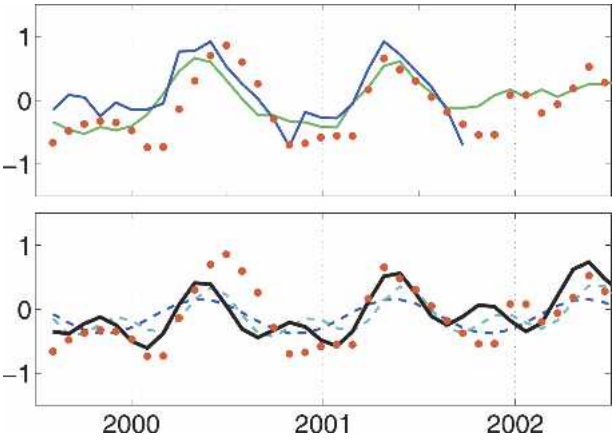

FIG. 3. As in Fig. 2, for just the TAO buoy at 140°W on the equator.

Adding 0.1 m s^{-1} everywhere to the altimeter estimates increases the skill to 30% (Table 1). Despite the strong qualitative resemblance between CWDs and altimeter estimators from 2°S to 2°N, skill (28%) is not higher there than for the overall average because two buoys (2°N, 180° and 2°N, 125°W) have large biases between the CWDs and the drifter mean.

The biases between the CWDs and the current estimators may result from an error in the scatterometer or TAO wind speed, interannual variations in currents (not parameterized by the SOI), or vertical shear in the water column. Because winds in the TAO array are predominantly westward, the bias would correspond to QuikSCAT wind speeds, being on average 0.1 m s^{-1} higher than the TAO winds, after accounting for currents, a relatively small error and well within the expected measurement errors of either. Alternatively, if the bias is from vertical shear, then the zonal surface currents are more eastward (generally, weaker) than the currents at 15 m.

The coefficients used for the altimeter estimator are given in Table 2 for each TAO buoy. The coefficients include the drifter mean plus 0.1 m s^{-1}. An estimator for the zonal surface currents, U_s, needed to correct zonal anemometer winds U in air–sea flux bulk formulas or for scatterometer–buoy comparisons, can be constructed for any time using (4) and these coefficients.

TABLE 1. Skill of estimators.

Data for estimator	Skill
Drifters	0.23
Altimeter + drifter mean	0.17
Altimeter + drifter mean + 0.1 m s^{-1}	0.30
Altimeter (2°S–2°N)	0.28

To obtain relative zonal motion, $U - U_s$, the estimate of U_s must be subtracted from the absolute (zonal) wind U (e.g., anemometer wind). The meridional component would be unchanged because, as discussed below, no meridional current estimator has significant skill.

6. Meridional velocities

Meridional CWDs are less predictable than their zonal counterparts but equally energetic. The overall rms values for the zonal and meridional CWDs are 0.41 and 0.43 m s^{-1}, respectively. The meridional analysis is difficult because the TIWs are probably overwhelming the mean, seasonal, or interannual components of the velocity. Geostrophic currents tend to be predominantly zonal, as are winds in the equatorial Pacific; thus, the Ekman component of the currents would be expected to be relatively large in this region. However, Ekman drift transitions to downwind drift approaching the equator, and this dynamical shift starts poleward of 2°N and 2°S. The meridional geostrophic current anomalies, in fact, are small and have no skill in estimating the meridional CWDs. The skill of the drifter estimates (which include an Ekman current component) is also quite small.

The means of the meridional CWDs for each buoy, plotted against the meridional drifter means (Fig. 4), show considerable scatter. Bin averaging the means by latitude reveals that meridional CWD means generally exceed drifter means by about a factor of 2 and that both estimates of mean currents are poleward, creating a mean divergence about the equator, as seen in Fig. 1. Ekman dynamics suggest that the surface velocities (corresponding to the CWDs) should be larger than those at 15 m (the drifter velocity depth); however, the magnitudes of the CWD vectors are larger than might be expected from an oceanic Ekman response (Ralph and Niiler 1999). We were unable to find systematic correlations between the time series of CWDs and wind stress that would indicate that they are in fact an Ekman response.

7. Application to scatterometer validation

In situ wind observations are routinely used to validate the empirical model function used to convert radar backscatter to wind vectors. Buoy winds have been used extensively in these efforts, and the TAO array contributes a large fraction of available buoy winds. Without a current correction, TAO buoy wind comparisons suggest that the QuikSCAT winds are too weak in the 3–10 m s^{-1} range, by the amount of the mean differences shown in Fig. 1a. This apparent bias

TABLE 2. Coefficients for zonal surface currents. Angles ϕ_1 and ϕ_2 are in radians. (Table is available online at http://ultrasat.apl.washington.edu/kkelly/ovwst.)

Lat	Lon	c	a_1	ϕ_1	a_2	ϕ_2	b	Lat	Lon	c	a_1	ϕ_1	a_2	ϕ_2	b
0°	137°E	0	0	0	0	0	0.46	8°S	155°W	0.01	0.06	1.59	0	0	−0.05
2°N	137°E	0.09	0.34	1.42	0.17	−0.41	−0.33	5°S	155°W	−0.14	0	0	0	0	−0.11
5°N	137°E	0.48	0.18	−1.14	0	0	0.02	2°S	155°W	−0.15	0.20	2.44	0.20	1.44	−0.15
8°N	137°E	−0.03	0.09	−1.07	0.07	2.82	0.06	0°	155°W	−0.04	0.23	−2.78	0.29	1.40	−0.25
0°	147°E	0.10	0.15	1.99	0.13	−0.29	−0.12	2°N	155°W	−0.24	0.45	−2.09	0.34	1.21	−0.26
2°N	147°E	0.12	0.19	2.10	0.14	−0.15	−0.17	5°N	155°W	0.18	0	0	0	0	−0.19
5°N	147°E	0.35	0.19	0.16	0	0	−0.07	8°N	155°W	0.31	0.34	0.11	1.01	−2.37	−0.01
5°S	156°E	0.01	0.09	1.12	0	0	−0.10	8°S	140°W	−0.05	0	0	0.05	−0.51	−0.07
2°S	156°E	−0.08	0.27	1.92	0.20	−0.14	−0.20	5°S	140°W	−0.16	0	0	0.08	1.89	−0.12
0°	156°E	0.13	0.23	2.40	0.24	0.20	−0.17	2°S	140°W	0.02	0.18	2.74	0.21	1.75	−0.10
2°N	156°E	0.05	0.23	2.52	0.21	0.25	−0.22	0°	140°W	0.01	0.26	−2.33	0.34	1.81	−0.24
5°N	156°E	0.30	0.18	0.52	0	0	−0.07	2°N	140°W	−0.30	0.50	−1.83	0.37	1.80	−0.26
8°N	156°E	0.09	0.19	−0.19	0.08	2.54	0.01	5°N	140°W	0.12	0	0	0.16	−0.15	−0.16
								9°N	140°W	0.19	0.27	1.04	0.06	3.14	−0.03
8°S	165°E	0.11	0.17	−0.72	0	0	0	8°S	125°W	−0.05	0.04	0.15	0	0	−0.07
5°S	165°E	0.02	0.14	1.54	0	0	−0.15	5°S	125°W	−0.21	0.09	0.09	0	0	−0.11
2°S	165°E	−0.09	0.32	2.21	0.25	0.24	−0.19	2°S	125°W	0.03	0.17	−3.10	0.19	1.73	−0.11
0°	165°E	0.08	0.27	2.82	0.28	0.40	−0.21	0°	125°W	−0.02	0.30	−1.99	0.28	2.12	−0.26
2°N	165°E	0.05	0.30	3.06	0.22	0.25	−0.29	2°N	125°W	−0.50	0.54	−1.55	0.30	2.45	−0.27
5°N	165°E	0.26	0.16	1.07	0	0	−0.10	5°N	125°W	0.08	0	0	0	0	−0.16
8°N	165°E	0.09	0.21	0.11	0.05	2.90	0.04	8°N	125°W	0.38	0.36	0.11	0.11	−0.24	−0.02
8°S	180°	0.06	0.12	0.17	0	0	−0.06	8°S	110°W	−0.08	0.08	0.06	0.05	−1.07	−0.06
5°S	180°	−0.05	0.11	1.92	0	0	−0.12	5°S	110°W	−0.22	0.08	0.48	0	0	−0.10
2°S	180°	−0.10	0.31	2.31	0.20	0.77	−0.18	2°S	110°W	0.07	0.17	−2.47	0.21	1.72	−0.15
0°	180°	−0.13	0.29	3.02	0.23	0.78	−0.26	0°	110°W	−0.06	0.40	−1.71	0.25	2.19	−0.28
2°N	180°	−0.19	0.38	−2.73	0.25	0.38	−0.31	2°N	110°W	−0.44	0.54	−1.29	0.18	2.46	−0.24
5°N	180°	0.25	0.15	0.94	0.10	−0.26	−0.14	5°N	110°W	0.23	0.19	0.18	0.21	−0.12	−0.12
8°N	180°	0.18	0.27	0.55	0.09	2.82	0.04	8°N	110°W	0.12	0.31	1.57	0	0	−0.04
8°S	170°W	0.04	0.10	0.77	0	0	−0.07	8°S	95°W	−0.02	0.05	0.34	0.05	0.15	−0.03
5°S	170°W	−0.11	0.10	2.17	0.08	1.09	−0.11	5°S	95°W	−0.11	0.06	−0.84	0.06	2.33	−0.08
2°S	170°W	−0.15	0.24	2.39	0.20	0.90	−0.14	2°S	95°W	0.01	0	0	0.16	2.07	−0.16
0°	170°W	−0.11	0.21	−3.06	0.27	0.90	−0.24	0°	95°W	−0.09	0.29	−1.22	0	0	−0.23
2°N	170°W	−0.25	0.37	−2.34	0.29	0.71	−0.27	2°N	95°W	−0.27	0.43	−0.98	0	0	−0.14
5°N	170°W	0.22	0	0	0	0	−0.15	3.5°N	95°W	0.07	0.29	−0.87	0	0	−0.09
8°N	170°W	0.27	0.33	0.76	0.08	−3.13	0	5°N	95°W	0.39	0	0	0.11	0.56	−0.07
								8°N	95°W	0.17	0.28	1.94	0.10	1.01	−0.01
								10°N	95°W	0.05	0.07	1.19	0	0	0.02
								12°N	95°W	0.03	0.16	−1.08	0.05	−2.87	0

could be even larger if a period of only a few months is used for the comparison; ocean currents can be as large as 1 m s^{-1} at many of the TAO buoy locations over a period of several months.

To illustrate the importance of removing the currents, we compared daily TAO winds with wind vectors from the SeaWinds scatterometer on the Japanese Midori (*ADEOS-II*) satellite. Calibration and preliminary validation of the SeaWinds instrument was based on only a few months of data (F. Wentz and D. Smith 2003, personal communication) (Fig. 5). These efforts require a timely comparison, which may preclude the availability of simultaneous current measurements. Therefore, the climatological estimators are particularly relevant for this application.

For three TAO buoys along 155°W (Fig. 5), SeaWinds data within 25 km were screened for rain and data from the problematic outer swath edges were eliminated. Nearby screened data from a single swath (up to four vectors) were averaged, and then the time series of vectors were filtered using the 5-day running mean. The TAO anemometer winds were also filtered using a 5-day running mean. Zonal scatterometer winds were subtracted from zonal TAO winds, and the CWDs were filtered using a 2-month running mean. At each buoy we used the coefficients in Table 2 and Eq. (4) to compute an estimate of the zonal current. The SOI (available from ftp://ftp.bom.gov.au/anon/home/ncc/www/sco/soi/soiplaintext.html, divided by 10) is customarily boxcar averaged over 5 months; for this ex-

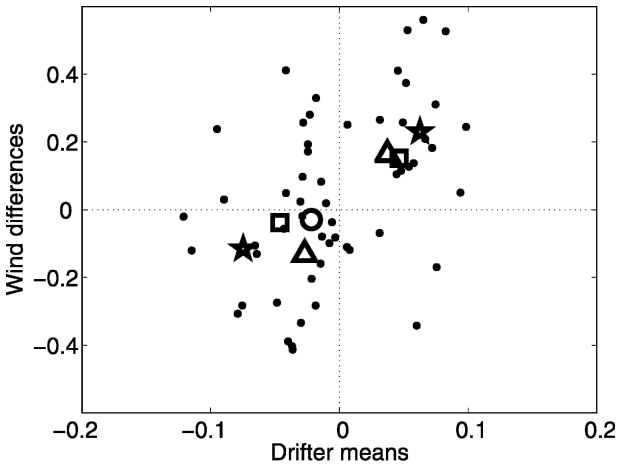

FIG. 4. Meridional wind differences vs drifters. Temporal average at each buoy (dots). Means binned by latitude at 8° (triangles), 5° (squares), 2° (stars), and at the equator (circle). Meridional velocities are generally poleward, with wind differences exceeding drifter means by a factor of 2.

ample, we averaged the SOI over the 5-month period spanning the observations. For each buoy the smoothed CWDs are shown (solid) along with the climatological current estimate (dashed). In all cases the mean westward current and its seasonal variations reproduce qualitatively the smoothed CWDs.

8. Conclusions

We compared 3-yr mean and monthly zonal surface currents in the tropical Pacific Ocean with collocated differences between absolute winds measured from anemometers on TAO buoys and relative winds measured by the satellite-based QuikSCAT scatterometer. Mean zonal CWDs resemble the mean currents from 15-m deep drifters; however, mean meridional CWDs are much larger than mean meridional drifter currents. The divergence of the mean CWDs (Fig. 1) about the equator is suggestive of an Ekman response.

Between 2°S and 2°N, where currents are relatively large, collocated wind differences (CWDs) agree qualitatively with near-surface currents from ADCP, current meters, and monthly surface geostrophic current anomalies from the TOPEX/Poseidon altimeter. At higher latitudes, the agreement is less clear.

The CWDs are also compared with climatological current estimators from drifters at 15-m depth, shipboard ADCP, and the geostrophic currents. Climatological estimators are used for drifter and ADCP data, owing to relatively sparse spatial and temporal sampling. The estimators consist (where available) of a mean, an annual, and a semiannual harmonic, and a factor related to the Southern Oscillation index (SOI). The drifter and ADCP magnitudes are considerably smaller than those of the altimeter and the CWDs, apparently the result of spatial smoothing. There is a significant reduction in CWD variance (skill) by subtracting either the altimeter or drifter estimators. However, the ADCP estimator does not significantly reduce the variance. There is a mean bias between the drifters and the CWDs, with drifters approximately 0.1 m s^{-1} more westward. It cannot be determined from these data whether this bias is from the winds or from the currents.

Meridional wind data and estimators show poor agreement with the meridional CWDs, consistent with previous unsuccessful attempts by Johnson et al. (2002) to characterize the meridional currents. Large, but unpredictable, currents have been attributed primarily to tropical instability waves. The meridional CWDs here have magnitudes nearly as large as the zonal component.

We provide (Table 2) the coefficients necessary to construct time-varying zonal current estimates at most TAO buoy locations: amplitudes and phases of the annual and semiannual harmonics, as well as the SOI regression coefficient from the altimeter data and the mean from the drifter data. When subtracted from an absolute (zonal) wind measurement, these time-varying surface current estimators give an estimate of relative motion, comparable to a scatterometer wind. The relative motion can be used to correctly implement bulk formulas (e.g., Liu et al. 1979) for computing air–sea fluxes, as well as to improve comparisons between scatterometer and buoy winds. This procedure could be

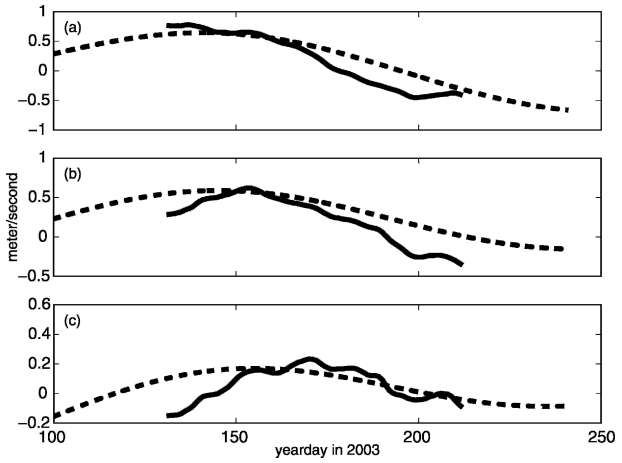

FIG. 5. Example of estimator for SeaWinds on the Midori satellite. Zonal component of daily TAO buoy wind minus scatterometer wind (solid) from SeaWinds on Midori and altimeter estimator (dashed) along 155°W at (a) 2°N, (b) the equator, and (c) 2°S.

extended to buoys in other regions in a straightforward fashion, provided altimetric SSH and an estimate of the mean current are available.

Acknowledgments. We thank the QuikSCAT project and PO.DAAC for scatterometer winds, the TAO Project Office for buoy winds and other meteorological variables, Dudley Chelton and Michael Schlax at OSU for the altimeter data, and Remote Sensing Systems for SSM/I data collocated with QuikSCAT. Comments by anonymous reviewers helped improve the analysis and clarify the text. KAK and SD were supported by NASA's Ocean Vector Winds Science Team (Contract 1216233 with the Jet Propulsion Laboratory). GCJ was supported by the NOAA Office of Oceanic and Atmospheric Research and the NOAA Office of Global Programs.

REFERENCES

Bonjean, F., and G. S. E. Lagerloef, 2002: Diagnostic model and analysis of the surface currents in the tropical Pacific Ocean. *J. Phys. Oceanogr.,* **32,** 2938–2954.

Dickinson, S., K. A. Kelly, M. J. Caruso, and M. J. McPhaden, 2001: Comparisons between the TAO buoy and NASA scatterometer wind vectors. *J. Atmos. Oceanic Technol.,* **18,** 799–806.

Freitag, H. P., M. O'Haleck, G. C. Thomas, and M. J. McPhaden, 2001: Calibration procedures and instrumental accuracies for ATLAS wind measurements. NOAA Tech. Memo. OAR PMEL-119, NOAA/Pacific Marine Environmental Laboratory, Seattle, WA, 20 pp.

Huddleston, J. N., R. D. West, S. H. Yueh, and Y. T. Wu, 1996: Advanced techniques for improving wind direction ambiguity removal in scatterometry. *IGARSS '96: Remote Sensing for a Sustainable Future*, New York, NY, IEEE, 1718–1720.

Jerlov, N. G., 1953: Studies of the equatorial currents in the Pacific. *Tellus,* **5,** 308–314.

Johnson, G. C., 2001: The Pacific Ocean subtropical cell surface limb. *Geophys. Res. Lett.,* **28,** 1771–1774.

——, B. M. Sloyan, W. S. Kessler, and K. E. McTaggart, 2002: Direct measurements of upper ocean currents and water properties across the tropical Pacific Ocean during the 1990's. *Progress in Oceanography,* Vol. 52, Pergamon, 31–61.

Kelly, K. A., S. Dickinson, and Z.-J. Yu, 1999: NSCAT tropical wind stress maps: Implications for improving ocean modeling. *J. Geophys. Res.,* **104C,** 11 291–11 310.

——, ——, M. J. McPhaden, and G. C. Johnson, 2001: Ocean currents evident in satellite wind data. *Geophys. Res. Lett.,* **28,** 2469–2472.

Lagerloef, G. S. E., G. T. Mitchum, R. B. Lukas, and P. P. Niiler, 1999: Tropical Pacific near-surface currents estimated from altimeter, wind and drifter data. *J. Geophys. Res.,* **104,** 23 313–23 326.

Liu, W. T., K. B. Katsaros, and J. A. Businger, 1979: Bulk parameterization of air–sea exchanges of heat and water vapor including the molecular constraints at the interface. *J. Atmos. Sci.,* **36,** 1722–1735.

Quilfen, Y., B. Chapron, and D. Vandemark, 2001: The ERS scatterometer wind measurement accuracy: Evidence of seasonal and regional biases. *J. Atmos. Oceanic Technol.,* **18,** 1684–1697.

Ralph, E. A., and P. P. Niiler, 1999: Wind-driven currents in the tropical Pacific. *J. Phys. Oceanogr.,* **29,** 2121–2129.

Sandwell, D. T., 1987: Biharmonic spline interpolation of GEOS-3 and Seasat altimeter data. *Geophys. Res. Lett.,* **14,** 139–142.

Wentz, F. J., and D. K. Smith, 1999: A model function for the ocean-normalized radar cross section at 14 GHz derived from NSCAT observations. *J. Geophys. Res.,* **104,** 11 499–11 514.

Yu, L., R. A. Weller, and B. Sun, 2004: Improving latent and sensible heat flux estimates for the Atlantic Ocean (1988–99) by a synthesis approach. *J. Climate,* **17,** 373–393.